Proteome analysis of human substantia nigra in Parkinson's disease

Manuela Basso[1 *], Sabrina Giraudo[2 *], Davide Corpillo[3], Bruno Bergamasco[2, 4], Leonardo Lopiano[2] and Mauro Fasano[1]

[1]Department of Structural and Functional Biology, and Center of Neuroscience, University of Insubria, Busto Arsizio, Italy
[2]Department of Neuroscience, University of Torino, Torino, Italy
[3]Bioindustry Park Canavese, Colleretto Giacosa, Italy
[4]Salvatore Maugeri Foundation, Pavia, Italy

Protein expression has been compared in human substantia nigra specimens from Parkinson's disease (PD) patients and from controls, and 44 proteins expressed in this midbrain region were identified by peptide mass fingerprinting. Among them, nine showed changes in their abundance. L and M neurofilament chains are less abundant in PD specimens, whereas peroxiredoxin II, mitochondrial complex III, ATP synthase D chain, complexin I, profilin, L-type calcium channel δ-subunit, and fatty-acid binding protein are significantly more present in PD samples than in controls. Besides the consolidated view of oxidative stress involvement in PD pathogenesis, suggested by overexpression of mitochondrial and reactive oxygen species (ROS)-scavenging proteins, these results indicate a possible potentiation mechanism of afferent signals to substantia nigra following degeneration of dopaminergic neurons.

Keywords: Excitotoxicity / Mitochondrial impairment / Oxidative stress / Parkinson's disease / Protein expression

Received: February 24, 2004; revised: April 6, 2004; accepted: April 13, 2004

1 Introduction

Parkinson's disease (PD) is the second most common neurodegenerative disorder after Alzheimer's disease (AD), with a prevalence of about 2% among people over the age of 65 years [1, 2]. The characteristic motor symptoms are associated with the depletion of dopaminergic melanin-containing neurons in the substantia nigra pars compacta (SNpc) and a consequent loss of dopamine in the striatum [1]. Another important pathological feature is the presence, especially in SNpc neurons, of eosinophilic cytoplasmic inclusion bodies (Lewy bodies, LB) [1, 3, 4]. LB show a strong staining with anti-α-synuclein antibodies [5], a presynaptic protein involved in a familial form of the disease [6, 7], present as the main filamentous component [8–10]. *In vitro* studies showed that both mutated and wild-type α-synucleins do form fibrils similar to those of LB; moreover, α-synuclein molecules carrying either one of the two point mutations observed in the familial PD will aggregate faster than the wild-type protein [11–13]. Recently, the effects of changes in the α-synuclein sequence on the enhanced susceptibility of cells to reactive oxygen species (ROS) have been reported [14–17], providing a pathogenic link between α-synuclein anomalies and a putative role of ROS in the cell death mechanisms in PD [18–21].

Substantia nigra (SN) is a preferential candidate to oxidative damage, since it contains oxidizable dopamine, neuromelanin, polyunsaturated fatty acids, iron, and relatively low antioxidant complement [21]. In this context, mitochondria are involved in a number of cellular reactions that potentially lead to the formation of ROS, like superoxide anions, hydroxyl radicals, and hydrogen peroxide. Complexes I and III in particular are associated with superoxide production, and the inhibition of these complexes results in increased free radical production. Mito-

Correspondence: Mauro Fasano, Center of Neuroscience, University of Insubria, via Alberto da Giussano 12, I-21052 Busto Arsizio (VA), Italy
E-mail: mauro.fasano@uninsubria.it
Fax: +39-0331-339459

Abbreviations: AD, Alzheimer's disease; **LB**, Lewy bodies; **PD**, Parkinson's disease; **ROS**, reactive oxygen species; **SN**, substantia nigra

* These authors contributed equally.

chondria contain antioxidant defence systems, such as glutathione, catalase, and superoxide dismutase, to carefully balance free radical production and detoxification. Oxidative stress is believed to be important in the ageing process and details of how ROS are produced from various intra- and extracellular sources as well as the cellular defence mechanisms and responses to oxidative stress have recently been extensively reviewed [22, 23].

Nowadays, the occurrence of a tight association of proteins to form insoluble supramolecular aggregates is considered to be the basis of a number of neurological diseases, both familial and sporadic. Self-aggregation of α-synuclein, wrong folding of the prion protein, defective cleavage of the amyloid β-peptide and hyperphosphorylation of the tau protein all lead to changes in the dynamics of cytosolic proteins and eventually the formation of macroscopic aggregates in PD, spongiform encephalopathy, and AD, respectively [8, 24]. An analysis of the water dynamics in *ex vivo* specimens of SNpc has shown a differential deposition of cytosolic proteins with respect to age-matched controls [25]. It has recently been proposed that misfolded α-synuclein could form channels in dopamine storage vesicles, thus contributing to the formation of cytoplasmic ROS due to dopamine oxidative catabolism [26].

In the present work, we describe a proteomic analysis of SN tissue in order to evaluate changes in the expression level of proteins that could provide information on the pathogenetic mechanism and on the pathways herein involved. To this purpose, we performed a two-dimensional electrophoretic (2-DE) separation of proteins extracted from *ex vivo* specimens from controls and PD patients. Forty-four proteins have been identified by peptide mass fingerprinting and their expression levels have been compared and statistically evaluated. Among them, nine proteins showed differential expression in PD patients respect to age-matched controls.

2 Materials and methods

2.1 Chemicals

Immobilized pH gradient (IPG) strips, IPG buffer, acrylamide, and Coomassie Brilliant Blue R-250 were purchased from Amersham Biosciences (Uppsala, Sweden). Modified trypsin was from Promega (Madison, WI, USA). ZipTip$_{C18}$ were from Millipore (Bedford, MA, USA). The protease inhibitor mix (from Sigma Chemical, St. Louis, MO, USA) contained 4-(2-aminoethyl)benzenesulfonyl fluoride (AEBSF), pepstatin A, *trans*-epoxysuccinyl-L-leucylamido(4-guanidino)butane (E-64), bestatin, leupeptin, and aprotinin, and was used according to manufacturer's instructions. All other chemicals were obtained from Sigma Chemical and used without further purification.

2.2 Tissues

Specimens of human SN from four patients having known PD history (sex 3 M, 1 F, aged 75 ± 3 years; deceased 13 ± 2 years after diagnosis; *postmortem* delay 4 h 38 min ± 26 min; brain weight 1156 ± 94 g) were provided by the Nederlandse Hersenbank (the Netherland's Brain Bank), Amsterdam. Each specimen was accompanied by histopathological report, showing depletion of pigmented dopaminergic neurons and the occurrence of extracellular neuromelanin granules as well as LB in surviving neurons. Four control specimens (sex 3 M, 1 F, aged 70 ± 8 years; *postmortem* delay 6 h 19 min ± 1 h 11 min; brain weight 1441 ± 127 g), not affected by neurodegenerative disorders, have been obtained from the same brain bank, also with histopathological report. SN have been excised from thawed autoptic specimens in order to refine the region of interest by cutting the surrounding unpigmented area using ceramic tools to avoid metal contamination of the samples. For less-pigmented PD tissues, a corresponding area has been removed. When present, blood clots have been removed before sample processing.

2.3 Protein extraction

Specimens (0.5–0.7 g) were homogenized (20 up-and-down strokes with a Teflon homogenizer followed by five passages through a 22-gauge needle) in 3 μL lysis solution (7 M urea, 2 M thiourea, 4% v/v CHAPS, 0.05 μL protease inhibitor mix) *per* mg tissue. After centrifugation at 21 000 × *g* for 30 min at 20°C supernatants were recovered; protein content was estimated with the 2D-Quant kit (Amersham Biosciences).

2.4 2-DE and data analysis

2-DE was performed according to Jacobs [27], with some modifications. Samples (~ 1 mg for Coomassie staining, ~ 100 μg for silver staining) were diluted to 250 μL with a buffer containing 7 M urea, 2 M thiourea, 4% CHAPS, 0.5% IPG buffer 3–10, 2 mM tributylphosphine, and traces of bromophenol blue and loaded onto 13 cm IPG DryStrips with a nonlinear pH 3–10 gradient by in-gel rehydration (1 h at 0 V, 10 h at 30 V). IEF was performed at 16°C on an IPGphor (Amersham Biosciences) according to the following schedule: 1 h at 200 V, 30 min of a linear gradient to 3500 V, 3 h at 3500 V, 2.5 h of a linear gradient to 8000 V, 6 h at 8000 V. Prior to SDS-PAGE, the IPG strips were equilibrated for 2 × 30 min in 50 mM Tris-HCl, pH 8.8, 6 M urea, 30% glycerol, 2% SDS, and traces of bromophenol blue containing 1% DTT for the first equilibration step and 2.5% iodoacetamide for the second one. SDS-PAGE was performed using 12.5% T, 2.6% C 1.5 mm thick separating polyacrylamide gels without stacking gel, using a Hoefer

SE 600 system (Amersham Biosciences). The second dimension was carried out at 45 mA/gel at 16°C and was terminated when the bromophenol dye front had migrated to the lower end of the gels. Carbamylated p*I* calibration markers (Amersham Biosciences) and molecular mass marker proteins (14–66 kDa from Sigma Chemical) were used for calibration of the molecular mass. The gels were stained either with Coomassie Brilliant Blue R-250 or according to Sinha's silver staining method [28]. After staining, gels were scanned with the ImageMaster Labscan V3.0 (Amersham Biosciences) and images were analyzed with ImageMaster 2D Elite V4.01 software package (Amersham Biosciences). Coomassie-stained spots were quantified on the basis of their relative volume (the spot volume divided by the total volume over the whole set of gel spots) and statistically analyzed according to the nonparametric Wilcoxon test. Relationships were considered statistically significant when $p < 0.05$.

2.5 Tryptic digestion of 2-DE gel spots

Coomassie-stained spots were manually excised and destained overnight with 40% ethanol in 25 mM ammonium bicarbonate. Gel pieces were washed twice with 25 mM ammonium bicarbonate and desiccated three times with acetonitrile. Each piece was then reswollen in 25 mM ammonium bicarbonate containing 1.2 μg of modified porcine trypsin and digestion proceeded overnight at 37°C. Peptides were extracted by sonication in 25 mM ammonium bicarbonate and loaded on $ZipTip_{C18}$.

2.6 MALDI-TOF-MS

Each peptide sample was eluted from $ZipTip_{C18}$ with a saturated solution of α-cyano-4-hydroxycinnamic acid in 70% acetonitrile and 0.2% TFA and 0.5 μL was spotted directly on a MALDI target plate. MALDI mass spectra were acquired in the positive reflectron ion mode with delayed extraction on a Reflex III time of flight instrument (Bruker Daltonics, Bremen, Germany) equipped with a 337 nm nitrogen laser. Ion acceleration voltage was set to 20.00 kV, the reflector voltage was set to 23.00 kV and the first extraction plate was set to 17.05 kV. Mass spectra were obtained by averaging 600 laser shots. Calibration of the spectra was performed internally by a two-points linear fit, using the autolysis products of trypsin at *m/z* 842.50 and 2211.10.

2.7 Database search

Database search with the peptide masses was performed against the Swiss-Prot database using the PeptIdent search algorithm (http://www.expasy.ch/tools/peptident.html). Mass tolerance for the monoisotopic peptide masses was set to 50 ppm.

3 Results

Proteins were extracted from four control specimens and four PD specimens, and analyzed in parallel by 2-DE, using both Coomassie Brilliant Blue and silver staining. With silver staining 50–100% more spots could be visualized (Fig. 1). By considering all the data sets, no significant differences were found between controls and PD patients in terms of appearance, disappearance or shift of any spot, with both staining methods.

In order to investigate how the overall expression of proteins is potentially affected in PD with respect to controls, 142 spots were selected for further analysis from the Coomassie-stained gels. Only spots that were mostly expressed or better focalized were chosen. In both specimens, the amount of protein present in each spot was densitometrically measured and statistically evaluated. Table 1 (see Addendum) reports isoelectric points and molecular weights, as deduced from the gel, and statistical analysis of spot volumes, according to Wilcoxon test, for each protein. Figure 2 shows the position of the 142 spots in a Coomassie-stained gel from a control specimen.

To build a map of the proteins extracted from human SN specimens, we tried to identify by peptide mass fingerprinting the spots that had been selected for statistical analysis. Spots were excised, both from control and PD gels, and digested with trypsin. Peptide masses were

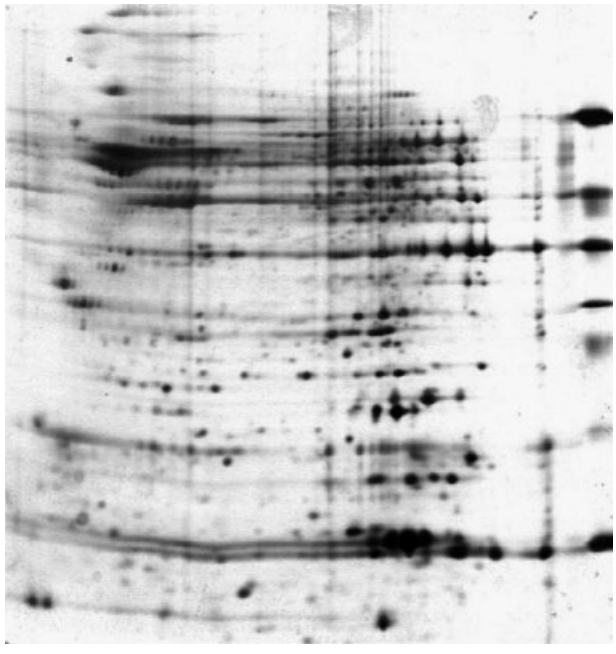

Figure 1. Silver-stained 2-DE gel of proteins extracted from an autoptic SN specimen of a control patient.

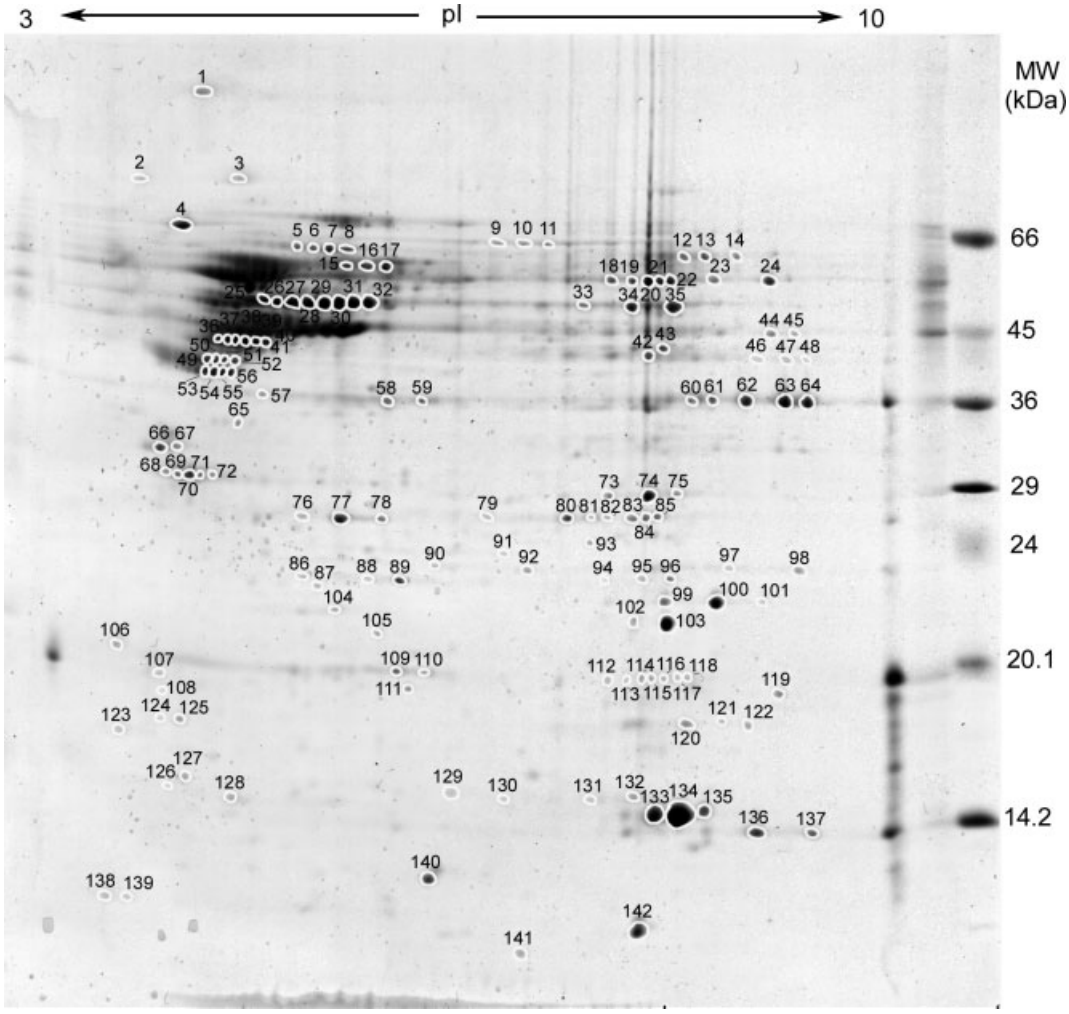

Figure 2. Coomassie-stained 2-DE gel of proteins extracted from an autoptic SN specimen of a control patient. Spots are labeled according to Table 1.

used to query the database. In order to evaluate protein identifications, we considered not only the percentage of sequence coverage (at least 20%), as indicated in Table 1, but also the number of matching peptides (at least five) and the gap between the accepted protein and the first excluded one in the list of candidates provided by the database search (at least a difference of three peptides). The procedure was successful, and 44 proteins were identified.

As it can be noticed from Table 1 (Addendum), nine of the 44 proteins are differentially expressed in PD tissues with respect to controls ($p < 0.05$). L and M neurofilament chains (spots 4 and 1, respectively) are less abundant in PD specimens, which is in keeping with degeneration of SNpc neurons. The other seven proteins, namely peroxiredoxin II (spot 89), mitochondrial complex III (spots 91 and 93), ATP synthase D chain (spot 87), complexin I (spot 127), profilin (spot 129), L-type calcium channel δ-subunit (spot 123), and fatty-acid binding protein (spot 130), are significantly more expressed in PD samples than in controls.

4 Discussion

Proteomics is a powerful methodology to investigate how protein expression is affected in the pathogenesis of a disease process. Nevertheless, there are to date a limited number of reports in the field of neurodegenerative disorders compared to other classes of diseases [29]. One of the limits of the technique is the limited number of protein spots that can be visualized on a single gel. Only the most expressed proteins are recognized, and very large or very small proteins cannot be adequately resolved. Also the range of p*I* values is a matter of concern; although nonlinear pH gradients are

commonly used, proteins having extreme p*I* values cannot focalize properly. Moreover, hydrophobic membrane proteins are difficult to resolve. Nonetheless, information on major proteins may also be of use, mainly for those proteins involved in the energetic metabolism of the cell. In a preliminary report, we observed that (mitochondrial) Mn-SOD and dihydropteridine reductase were increased twofold in PD with respect to controls, although specimen variability did not allow to have statistically significant figures [30].

Among the 44 proteins identified in this work, nine show significant changes in their level of expression. In particular, higher expression of peroxiredoxin II is in agreement with the oxidative stress hypothesis in PD [18, 23]. Peroxiredoxin II has been recently reported to be more expressed in the frontal cortex of PD, AD, and Down syndrome patients [31]. Peroxiredoxins are sacrificial antioxidants, *i.e.*, instead of catalyzing ROS oxidation/reduction they react themselves with ROS. In this process, available protein thiols (Cys-SH) are oxidized to sulfinyl residues (Cys-SO_2^-) with a consequent reduction of the p*I*. To the peroxiredoxin family belongs the DJ-1 protein as well; recently, a large deletion in the DJ-1 gene was reported to cosegregate with early-onset PD in a consanguineous Dutch family; moreover, a L166P mutation was found in an Italian family [32]. DJ-1 is known to interact with c-myc and to increase cell transformation, and to inhibit the RNA-binding ability of a cAMP-responsive multiprotein complex that includes glyceraldehyde-3-phosphate dehydrogenase [19]. It has also been supposed that DJ-1 acts as a ROS scavenger, thus modulating oxidant stress conditions. DJ-1 behaves as a hydroperoxide-responsive protein, that is converted into a variant with a more acidic p*I* in response to oxidative stress, suggesting a function as an antioxidant protein [33, 34]. These authors also described a similar behavior for peroxiredoxins in the case of human umbilical vein endothelial cells in response to oxidative stress [35].

Actually, there are suggestions that ROS, by-products of the oxidative metabolic pathway, may damage cell membranes through addition to unsaturated bonds in the lipid bilayer [18]. Oxidant stress conditions may, in turn, be strictly connected to excitotoxicity or to mitochondrial dysfunction [23, 36].

A reduced complex I activity was first identified in the SN of *post mortem* PD brain [23, 37]. Other brain areas showed normal oxidative phosphorylation activity [23, 37, 38]. Complex I defect is specific to PD and selective for the SN, but not related to the formation of LB [23]. Additional defects in complexes II and III were reported as well [39, 40]. Mitochondrial changes in PD could either be the result from inherited mutations in the mitochondrial respiration proteins or a consequence of environmental factors and/or sporadic somatic mutations that compromise normal mitochondrial activity [23]. We report that mitochondrial complex III (ubiquinol cytochrome *c* reductase) shows a two- to threefold increase on two independent spots, and mitochondrial complex V (ATP synthase) has a twofold higher abundance in PD specimens. Therefore, lower activity previously reported in the literature should be related to the inhibition of mitochondrial enzymes in PD rather than a reduction in their expression level; thus, the increased expression observed here could be related to a compensatory mechanism. In both approaches, however, it is not possible to distinguish the contribution of nigral neurons from that of glial cells in SNpc homogenates.

Complexin I, profilin, and L-type calcium channel δ subunit all appear to be more expressed in PD patients. Complexins are particularly abundant in presynaptic terminals, where they play an important role in modulating neurotransmitter release by exocytosis [41]. It has been suggested that complexin overexpression could enhance the probability of vesicle fusion upon influx of Ca^{2+} ions by increasing the number of vesicles close to full fusions.

It appears of peculiar interest the fact that L-type channels are more expressed in PD, as it was reported for hippocampus specimens from AD patients [42]. Increased density of L-type Ca^{2+} channels was actually associated to selective neuronal death in hippocampus in AD. These channels allow Ca^{2+} influx after a change in membrane potential due to glutamate binding to AMPA/kainate receptors. Also in PD, the increase of calcium influx might constitute an additional risk factor for involved neurons.

Actually, most of the results described here concern presynaptic proteins; since our specimens are composed by mesencephalic SN, the findings described are probably related to modifications of afferent fibers to nigral dopaminergic neurons as a consequence of the extensive SN cell death. In this view, two possible considerations could be made: first, the increase of presynaptic proteins in afferent terminals could be a mechanism to increase dopamine release by nigrostriatal neurons; second, this possible afferent hyperactivity could also involve glutamatergic fibers from subthalamic nucleus, supporting, at least partially, the excitotoxic hypothesis for SN degeneration [43]. Concerning profilin, it is a cytoskeleton-interacting protein that binds to actin monomers resulting in cytoskeletal changes. This finding could therefore be suggestive of modifications of neurofilaments at the SNpc level that takes place during the neurodegenerative process of PD. Unlike a similar work on AD brain areas [44], cytoplasmic Cu,Zn-SOD (spot 109) and α-crystallin B chain (spots 102 and 103) do not appear here to be pres-

ent in increased amount in PD SN tissue with respect to the controls. Ubiquitin (spot 142) appears in all maps with comparable intensities. This aspect has to be related to the hypothesis that an impairment in UCH-L1 activity [45], that would reduce the availability of ubiquitin monomers for further ubiquitin tagging of proteins to be degraded, is a minor factor in sporadic PD [46].

In conclusion, we have identified proteomic coordinates of 44 proteins expressed in human SN and a comparison between controls and PD patients have been made. Our findings are consistent with the view of oxidative stress involvement in PD pathogenesis, as suggested by over-expression of mitochondrial and ROS-scavenging proteins. Moreover, our work provides information about a possible potentiation mechanism of afferent signals to SN following degeneration of dopaminergic neurons. Finally, this extensive application of the proteomic approach to understand the molecular basis of PD demonstrates the great potentiality of this methodology in the field of neurodegenerative disorders.

The authors thank Professor Riccardo Fesce for helpful discussion. We gratefully acknowledge Fondazione Cavalieri Ottolenghi, Torino, Italy and Fondazione Monzino, Milano, Italy for financial support.

5 References

[1] Lang, A. E., Lozano, A. M., *New Engl. J. Med.* 1999, *339*, 1044–1053.

[2] Martin, J. B., *New Engl. J. Med.* 1999, *340*, 1970–1980.

[3] Lewy, F. H., in: Lewandowsky, M., Abelsdorff, G. (Eds.), *Handbuch der Neurologie Band III*, Springer, Berlin 1912, pp. 920–933.

[4] Galvin, J. E., Lee, V. M-Y., Schmidt, L., Tu, P-H., Iwatsubo, T., Trojanowski, J. Q., *Adv. Neurol.* 1999, *80*, 313–324.

[5] Spillantini, M. G., Schmidt, M. L., Lee, V. M., Lee, Y. *et al.*, *Nature* 1997, *388*, 839–840.

[6] Polymeropoulos, M. H., Lavedan, C., Leroy, E., Ide, S. E. *et al.*, *Science* 1997, *276*, 2045–2047.

[7] Krüger, R., Kuhn, W., Müller, T., Woitalla, D. *et al.*, *Nat. Genet.* 1998, *18*, 106–108.

[8] Schulz, J. B., Dichgans, J., *Curr. Op. Neurol.* 1999, *12*, 433–439.

[9] Golbe, L. I., *Mov. Disord.* 1999, *14*, 6–9.

[10] Goedert, M., *Nat. Rev. Neurosci.* 2001, *2*, 492–501.

[11] Narhi, L., Wood, S. J, Steavenson, S., Jiang, Y. *et al.*, *J. Biol. Chem.* 1999, *274*, 9843–9846.

[12] Wood, S. J., *J. Biol. Chem.* 1999, *274*, 19509–19512.

[13] Conway, K. A., Lee, S.-J., Rochet, J.-C., Ding, T. T. *et al.*, *Proc. Natl. Acad. Sci. USA* 2000, *97*, 571–576.

[14] Kanda, S., Bishop, J. F., Eglitis, M. A., Yang, Y., Mouradian, M. M., *Neuroscience* 2000, *97*, 279–284.

[15] Tabrizi, S. J., Orth, M., Wilkinson, J. M., Taanman, J. W. *et al.*, *Hum. Mol. Genet.* 2000, *9*, 2683–2689.

[16] Tanaka, Y., Engelender, S., Igarashi, S., Rao, R. K. *et al.*, *Hum. Mol. Genet.* 2001, *10*, 919–926.

[17] Junn, E., Mouradian, M. M., *Neurosci. Lett.* 2002, *320*, 146–150.

[18] Przedborski, S., Jackson-Lewis, V. R., in: Poli, G., Cadenas, E., Packer, L. (Eds.), *Free Radicals in Brain Pathophysiology*, Marcel Dekker, New York 2000, pp. 273–290.

[19] Cookson, M. R., *Neuron* 2003, *37*, 7–10.

[20] Ischiropoulos, H., Beckman, J. S., *J. Clin. Invest.* 2003, *111*, 163–169.

[21] Jenner, P., *Ann. Neurol.* 2003, *53* Suppl. 3, S26–S36.

[22] Finkel, T., Holbrook, N. J., *Nature* 2000, *408*, 239–247.

[23] Orth, M., Schapira, A. H., *Neurochem. Int.* 2002, *40*, 533–541.

[24] Borden, K. L., *Ann. Neurol.* 1998, *44*, S65–S71.

[25] Lopiano, L., Fasano, M., Giraudo, S., Digilio, G. *et al.*, *Neurochem. Int.* 2000, *37*, 331–336.

[26] Lotharius, J., Brundin, P., *Hum. Mol. Genet.* 2002, *11*, 2395–2407.

[27] Jacobs, D. I., van Rijssen, M. S., van der Heijden, R., Verpoorte, R., *Proteomics* 2001, *1*, 1345–1350.

[28] Sinha, P., Poland, J., Schnölzer, M., Rabilloud, T., *Proteomics* 2001, *1*, 835–840.

[29] Morrison, R. S., Kinoshita, Y., Johnson, M. D., Uo, T. *et al.*, *Mol. Cell. Proteomics* 2002, *1*, 553–560.

[30] Basso, M., Giraudo, S., Lopiano, L., Bergamasco, B. *et al.*, *Neurol. Sci.* 2003, *24*, 155–156.

[31] Krapfenbauer, K., Engidawork, E., Cairns, N., Fountoulakis, M., Lubec, G., *Brain Res.* 2003, *967*, 152–160.

[32] Bonifati, V., Rizzu, P., van Baren, M. J., Schaap, O. *et al.*, *Science* 2002, *199*, 256–259.

[33] Mitsumoto, A., Nakagawa, Y., Takeuchi, A., Okawa, K. *et al.*, *Free Radic. Res.* 2001, *35*, 301–310.

[34] Mitsumoto, A., Nakagawa, Y., *Free Radic. Res.* 2001, *35*, 885–893.

[35] Mitsumoto, A., Takanezawa, Y., Okawa, K., Iwamatsu, A., Nakagawa, Y., *Free Radic. Biol. Med.* 2001, *30*, 625–635.

[36] Pocernich, C. B., Cardin, A. L., Racine, C. L., Lauderback, C. M., Butterfield, D. A., *Neurochem. Int.* 2001, *39*, 141–149.

[37] Gu, M., Owen, A. D., Toffa, S. E. K., Cooper, J. M. *et al.*, *J. Neurol. Sci.* 1998, *158*, 24–29.

[38] Cooper, J. M., Daniel, S. E., Marsden, C. D., Schapira, A. H. V., *Mov. Disord.* 1995, *10*, 295–297.

[39] Mizuno, Y., Suzuki, K., Ohta, S., *J. Neurol. Sci.* 1990, *96*, 49–57.

[40] Mizuno, Y., Matuda, S., Yoshino, H., Moro, H. *et al.*, *Ann. Neurol.* 1994, *35*, 201–210.

[41] Marz, K. E., Hanson, P. I., *Trends Neurosci.* 2002, *25*, 381–383.

[42] Coon, A. L., Wallace, D. R., Mactutus, C. F., Booze, R. M., *Neurobiol. Aging* 1999, *20*, 597–603.

[43] Gu, B., Zhang, Y. D., Hu, G., *Neurosci. Lett.* 2003, *351*, 186–190.

[44] Schonberger, S. J., Edgar, P. F., Kydd, R., Faull, R. L. M., Cooper, G. J. S., *Proteomics* 2001, *1*, 1519–1528.

[45] Leroy, E., Boyer, R., Auburger, G., Leube, B. *et al.*, *Nature* 1998, *395*, 451–452.

[46] Harhangi, B. S., Farrer, M. J., Lincoln, S., Bonifati, V. *et al.*, *Neurosci. Lett.* 1999, *270*, 1–4.

6 Addendum

Table 1. Statistical analysis and identification of proteins from human SN of control subjects and PD patients

Spot	Controls (%)	PD (%)	Calculated p*I*	Calculated MW (kDa)	*p* Wilcoxon	Protein	Theoretical p*I*	Theoretical MW (kDa)	ID	% Seq. covered
1	6.632 ± 5.188	1.629 ± 1.410	4.462	119 637 64 446.37	0.002	Neurofilament M	4.90	102 316	P07197	28.6
2	1.365 ± 1.974	0.525 ± 0.483	4.245	83 313	0.331					
3	1.060 ± 0.856	0.775 ± 0.552	4.746	83 313	0.574					
4	6.867 ± 3.386	3.075 ± 1.741	4.462	69 118	0.001	Neurofilament L	4.66	61 646	P07196	43.6
5	0.285 ± 0.129	0.258 ± 0.158	5.050	63 521	0.689					
6	0.380 ± 0.215	0.420 ± 0.387	5.150	63 249	0.456					
7	0.378 ± 0.126	0.317 ± 0.126	5.222	62 979	0.438					
8	0.263 ± 0.109	0.195 ± 0.074	5.291	62 844	0.252					
9	0.186 ± 0.103	0.251 ± 0.121	6.186	64 623	0.867	Serum albumin	5.67	66 472	P02768	21.4
10	0.231 ± 0.141	0.345 ± 0.110	5.351	64 345	0.613					
11	0.159 ± 0.170	0.414 ± 0.226	6.514	64 207	0.152					
12	0.371 ± 0.520	0.290 ± 0.186	7.386	61 125	0.645	Pyruvate kinase, M2 isozyme	7.95	57 783	P14786	33.4
13	0.495 ± 0.329	0.547 ± 0.282	7.534	61 125	0.721					
14	0.328 ± 0.264	0.407 ± 0.206	7.780	61 386	0.235					
15	0.250 ± 0.149	0.184 ± 0.058	5.310	59 088	0.388					
16	0.279 ± 0.201	0.398 ± 0.172	5.406	58 840	0.541					
17	0.211 ± 0.084	0.382 ± 0.151	5.499	58 716	0.167					
18	0.371 ± 0.486	0.465 ± 0.185	6.924	55 956	1.427	Glu dehydrogenase 1, mitochondrial	6.71	56 009	P00367	21
19	0.447 ± 0.293	0.345 ± 0.139	7.049	55 840	1.257					
20	0.286 ± 0.076	0.353 ± 0.219	7.157	55 493	0.837					
21	0.341 ± 0.216	0.246 ± 0.150	7.224	55 608	0.955					
22	0.388 ± 0.158	0.390 ± 0.169	7.295	55 608	1.242					
23	0.491 ± 0.193	0.562 ± 0.214	7.591	56 073	0.808					
24	1.444 ± 1.157	1.270 ± 0.651	8.022	56 073	1.269	ATP synthase α-chain, mitochondrial	8.28	55 209	P25705	32.9
25	0.121 ± 0.091	0.172 ± 0.107	5.027	51 747	0.643	Glial fibrillary acidic protein, astrocyte	5.42	49 880	P14136	56.9
26	0.282 ± 0.185	0.310 ± 0.306	5.127	51 432	1.164					
27	0.398 ± 0.277	0.557 ± 0.375	5.029	51 016	0.613					
28	0.677 ± 0.399	0.511 ± 0.391	5.291	51 224	0.963					
29	1.199 ± 0.591	0.845 ± 0.574	5.393	51 224	0.114					
30	1.521 ± 0.736	0.930 ± 0.611	5.493	51 224	0.077					
31	1.319 ± 1.016	0.694 ± 0.393	5.583	51 224	0.222					
32	0.936 ± 0.747	0.589 ± 0.541	5.590	51 224	0.423					
33	0.750 ± 0.527	0.698 ± 0.390	6.734	50 913	1.175					
34	1.782 ± 0.547	1.904 ± 0.740	7.034	50 605	0.758					
35	1.229 ± 0.500	1.908 ± 0.779	7.036	50 503	0.114					
36	0.103 ± 0.059	0.069 ± 0.033	4.668	45 013	0.412					
37	0.154 ± 0.090	0.101 ± 0.007	4.718	44 838	0.230					
38	0.271 ± 0.188	0.123 ± 0.022	4.762	44 925	0.073					
39	0.271 ± 0.103	0.162 ± 0.057	4.810	44 838	0.073					
40	0.280 ± 0.113	0.192 ± 0.059	4.854	44 664	0.164					
41	0.315 ± 0.146	0.176 ± 0.044	4.908	44 491	0.257					
42	0.204 ± 0.097	0.298 ± 0.183	7.190	42 404	0.354	Fructose-bisphosphate aldolase C	6.46	39 325	P09972	36.1
43	0.253 ± 0.156	0.421 ± 0.193	7.261	43 640	0.222	Aspartate aminotransferase, cytoplasmic	6.57	46 116	P17174	38.1

Table 1. Continued

Spot	Controls (%)	PD (%)	Calculated p*I*	Calculated MW (kDa)	*p* Wilcoxon	Protein	Theoretical p*I*	Theoretical MW (kDa)	ID	% Seq. covered
44	0.495 ± 0.288	0.605 ± 0.247	8.033	46 081	0.435	Phosphoglycerate kinase 1	8.30	44 597	P00558	20.01
45	0.221 ± 0.194	0.453 ± 0.239	8.219	45 991	0.065					
46	0.136 ± 0.058	0.185 ± 0.092	7.935	42 163	0.435					
47	0.218 ± 0.083	0.268 ± 0.142	8.124	41 844	0.524					
48	0.111 ± 0.051	0.169 ± 0.094	8.271	41 765	0.435					
49	0.084 ± 0.031	0.075 ± 0.049	4.605	41 844	0.442					
50	0.154 ± 0.090	0.093 ± 0.068	4.652	41 765	0.235					
51	0.228 ± 0.127	0.141 ± 0.128	4.696	41 686	0.161					
52	0.218 ± 0.088	0.177 ± 0.164	4.746	41 607	0.645					
53	0.258 ± 0.097	0.168 ± 0.114	4.599	40 225	0.108					
54	0.301 ± 0.094	0.212 ± 0.124	4.643	40 075	0.154					
55	0.499 ± 0.163	0.321 ± 0.233	4.683	40 000	0.277					
56	0.274 ± 0.290	0.475 ± 0.289	4.734	40 075	0.148					
57	0.146 ± 0.085	0.169 ± 0.115	4.886	37 376	0.762					
58	0.148 ± 0.118	0.321 ± 0.126	5.493	36 513	0.073	Guanine nucleotide-binding protein β-subunit 1	5.60	37 377	P04901	27.6
59	0.255 ± 0.165	0.509 ± 0.258	5.731	36 513	0.053					
60	0.343 ± 0.297	0.268 ± 0.095	7.450	36 775	0.860	Glyceraldehyde 3-phosphate dehydrogenase	8.58	35 922	P04406	30.5
61	0.665 ± 0.384	0.548 ± 0.261	7.610	36 775	0.596					
62	1.146 ± 0.511	1.048 ± 0.764	7.865	36 578	0.331					
63	1.810 ± 0.580	1.770 ± 1.254	8.140	36 448	0.377					
64	1.479 ± 0.474	1.518 ± 0.712	8.327	36 318	0.724					
65	0.253 ± 0.180	0.354 ± 0.152	4.772	33 976	0.345					
66	0.290 ± 0.161	0.495 ± 0.276	4.385	31 699	0.161	14-3-3 protein ε	4.67	29 174	P42655	65.9
67	0.323 ± 0.314	0.295 ± 0.276	4.485	31 646	1.269					
68	0.136 ± 0.128	0.115 ± 0.072	4.486	29 327	1.245	14-3-3 protein γ	4.80	28 171	P35214	44.7
69	0.234 ± 0.191	0.251 ± 0.093	4.531	29 096	0.383					
70	0.294 ± 0.179	0.422 ± 0.251	4.533	29 188	0.336					
71	0.180 ± 0.081	0.272 ± 0.141	4.589	29 096	0.272					
72	0.119 ± 0.164	0.167 ± 0.152	4.655	29 142	0.083					
73	0.445 ± 0.239	0.557 ± 0.363	6.916	27 566	0.860	Phosphoglycerate mutase 1	6.75	28 672	P18669	38.3
74	2.247 ± 0.841	1.755 ± 0.581	7.183	27 525	0.190					
75	0.648 ± 0.116	0.461 ± 0.176	7.378	27 650	0.024					
76	0.378 ± 0.561	0.399 ± 0.307	5.144	26 057	1.530					
77	1.346 ± 0.810	1.763 ± 0.663	5.291	25 869	0.222	Ubiquitin thiolesterase L1	5.33	24 824	P09936	43
78	0.604 ± 0.702	0.663 ± 0.462	5.373	25 795	0.222					
79	0.274 ± 0.431	0.191 ± 0.082	6.140	26 019	0.366					
80	1.187 ± 0.739	1.436 ± 0.674	6.665	25 944	0.480	Dihydropteridine reductase	6.90	25.803	P09417	55.3
81	0.371 ± 0.240	0.318 ± 0.112	6.810	25 982	0.798					
82	0.219 ± 0.126	0.181 ± 0.060	6.920	25 982	0.681					
83	0.354 ± 0.287	0.552 ± 0.293	7.079	25 869	0.162					
84	0.358 ± 0.214	0.258 ± 0.114	7.187	25 869	0.673					
85	0.641 ± 0.334	0.562 ± 0.219	7.269	25 944	0.724					
86	0.132 ± 0.085	0.184 ± 0.078	5.144	21 759	1.242					
87	0.132 ± 0.100	0.232 ± 0.116	5.160	20 391	0.050	ATP synthase D chain, mitochondrial	5.22	18 360	O75947	63.7
88	0.426 ± 0.766	0.284 ± 0.112	5.439	21 685	1.059					
89	0.800 ± 0.330	1.596 ± 0.496	5.573	21 661	0.004	Peroxiredoxin 2	5.66	21 891	P32119	42.9
90	0.205 ± 0.223	0.271 ± 0.148	5.830	22 419	0.299					

Table 1. Continued

Spot	Controls (%)	PD (%)	Calculated p*I*	Calculated MW (kDa)	*p* Wilcoxon	Protein	Theoretical p*I*	Theoretical MW (kDa)	ID	% Seq. covered
91	0.073 ± 0.094	0.118 ± 0.029	6.277	23 210	0.043	Ubiquinol-cytochrome *c* reductase iron-sulfur subunit, mitochondrial	6.30	21 616	P47985	23.5
92	0.327 ± 0.240	0.428 ± 0.155	6.415	22 527	0.272					
93	0.152 ± 0.058	0.454 ± 0.125	6.803	24 387	0.003	Ubiquinol-cytochrome *c* reductase iron-sulfur subunit, mitochondrial	6.30	21 616	P47985	25
94	0.120 ± 0.141	0.153 ± 0.168	6.924	22 084	0.731	Superoxide dismutase [Mn]	6.86	22 204	P04179	21.7
95	0.300 ± 0.170	0.300 ± 0.172	7.149	22 135	1.000					
96	0.515 ± 0.303	0.752 ± 0.285	7.348	22 160	0.077					
97	0.161 ± 0.077	0.352 ± 0.107	7.753	22 912	0.121					
98	0.604 ± 0.341	0.941 ± 0.453	8.283	22 605	0.181	Peroxiredoxin 1	8.27	22 110	Q06830	37.2
99	1.120 ± 0.576	1.075 ± 0.566	7.299	21 303	0.596	α-crystallin B chain	6.76	20 159	O43416	35.6
100	3.777 ± 0.971	3.535 ± 0.691	7.675	21 140	0.930					
101	0.306 ± 0.166	0.292 ± 0.262	8.025	21 256	1.530	Phosphatidylethanolamine-binding protein	7.43	20 925	P30086	55.4
102	1.135 ± 0.680	0.926 ± 0.795	7.123	20 455	0.251	α-crystallin B chain	6.76	20 159	P02511	34.3
103	6.636 ± 1.345	6.027 ± 1.745	7.325	20 295	0.480					
104	0.211 ± 0.118	0.511 ± 0.262	5.160	20 391	0.114	Ferritin heavy chain	5.30	21.907	P02794	36.9
105	0.313 ± 0.294	0.771 ± 0.729	5.410	19 513	1.464					
106	0.336 ± 0.213	0.372 ± 0.247	4.181	19 498	0.943					
107	0.046 ± 0.031	0.111 ± 0.081	4.422	18 465	0.147					
108	0.146 ± 0.086	0.068 ± 0.054	4.437	17 951	0.111					
109	0.477 ± 0.341	0.585 ± 0.208	5.596	18 210	0.289	Superoxide dismutase [Cu-Zn]	5.70	15 804	P00441	49
110	1.032 ± 0.659	1.369 ± 0.682	5.752	18 241	0.480					
111	0.418 ± 0.197	0.409 ± 0.149	5.508	18 034	0.959	Stathmin	5.77	17 171	P16949	37.8
112	0.107 ± 0.087	0.340 ± 0.107	6.633	18 272	0.200	Myelin basic protein	6.00	21 522	P02686-2 (isoform)	24.4
113	0.037 ± 0.025	0.227 ± 0.169	6.693	18 324	0.095					
114	0.088 ± 0.090	0.271 ± 0.139	6.799	18 376	0.143					
115	0.084 ± 0.098	0.209 ± 0.092	6.946	18 359	0.381					
116	0.055 ± 0.057	0.157 ± 0.092	7.068	18 341	0.229					
117	0.335 ± 0.363	0.185 ± 0.030	7.172	18 324	1.600					
118	0.042 ± 0.010	0.191667	7.254	18 376	2.000					
119	0.577 ± 0.497	0.848 ± 0.529	8.160	17 870	0.351	Cofilin, non-muscle isoform	8.22	18 502	P23528	47
120	0.512 ± 0.287	0.815 ± 0.422	7.469	17 024	0.162	Peptidyl-prolyl *cis-trans* isomerase A	7.82	17 881	P05092	34.1
121	0.299 ± 0.399	0.300 ± 0.147	7.749	17 066	0.606					
122	0.304 ± 0.261	0.557 ± 0.389	7.943	16 996	0.077					
123	0.141 ± 0.081	0.377 ± 0.214	4.202	16 591	0.008	Chain 2: L-type calcium channel δ-subunit	4.47	16 466	P54289	36.7
124	0.060 ± 0.038	0.148 ± 0.091	4.431	16 850	0.065	Chain 1: factor X light chain	4.59	15 725	P00742	53.2
125	0.591 ± 0.398	0.807 ± 0.384	4.527	16 838	0.232					
126	0.132 ± 0.219	0.066 ± 0.054	4.462	15 654	0.876	Cytochrome *c* oxidase polypeptide Va, mitochondrial	4.88	12 513	P20674	36.7
127	0.093 ± 0.024	0.277 ± 0.152	4.540	15 835	0.008	Complexin 1	4.93	15 030	O14810	36.6
128	0.239 ± 0.140	0.431 ± 0.111	4.769	15 442	0.189	Galectin-1	5.34	14 584	P09382	60.4

Table 1. Continued

Spot	Controls (%)	PD (%)	Calculated p*I*	Calculated MW (kDa)	*p* Wilcoxon	Protein	Theoretical p*I*	Theoretical MW (kDa)	ID	% Seq. covered
129	0.059 ± 0.024	0.149 ± 0.068	5.926	15 541	0.010	Splice isoform IIB of Profilin II	5.81	14 957	P35080-2 (isoform)	33.1
130	0.044 ± 0.025	0.103 ± 0.037	6.287	15 422	0.008	Fatty acid-binding protein	6.34	14 727	P05413	40.2
131	0.265 ± 0.246	0.359 ± 0.197	6.858	15 402	0.114	Hemoglobin β-chain	6.81	15 867	P02023	87.7
132	0.373 ± 0.183	0.568 ± 0.066	7.138	15 481	0.006					
133	3.263 ± 0.663	3.633 ± 1.587	7.276	15 139	1.000					
134	10.542 ± 2.087	10.369 ± 4.734	7.446	15 130	0.190					
135	1.448 ± 0.564	1.811 ± 1.374	7.637	15 222	0.791					
136	4.941 ± 2.140	2.857 ± 0.796	8.022	14 886	1.829	Hemoglobin α-chain	8.73	15 126	P01922	83.7
137	4.816 ± 2.614	3.471 ± 2.445	8.496	14 861	1.655					
138	0.156 ± 0.128	0.271 ± 0.156	4.103	14 041	0.284	Thioredoxin	4.82	11 606	P10599	46.2
139	0.104 ± 0.079	0.272 ± 0.252	4.232	14 041	0.214					
140	1.580 ± 0.935	1.234 ± 0.431	5.782	14 240	0.743	Cytocrome *c* oxidase polypeptide VIb	6.79	10 061	P14854	89.4
141	0.143 ± 0.034	0.308 ± 0.145	6.376	7000	0.111	Chain 2: neuregulin-4	5.46	6663	Q8WWG1	50.8
142	3.762 ± 1.089	3.630 ± 1.055	7.175	13 699	1.057	Ubiquitin	7.99	9071	Q15843	65.8

